



Die filling optimization using three-dimensional discrete element modeling

C. Bierwisch*, T. Kraft, H. Riedel, M. Moseler

Fraunhofer-Institut für Werkstoffmechanik IWM, Wöhlerstraße 11, 79108 Freiburg, Germany

ARTICLE INFO

Article history:

Received 28 January 2009

Received in revised form 21 July 2009

Accepted 22 July 2009

Available online 6 August 2009

Keywords:

Die filling

Density distribution

Density homogeneity index

Discrete element method

Coarse graining

ABSTRACT

Inhomogeneous density distributions after die filling are a ubiquitous problem in powder technological part production. In this paper, numerical simulations of the die filling process in realistic, three-dimensional (3D) cavities are presented using the discrete element method with both multi-sphere and single sphere grain models. Good agreement was found between calculated and experimentally measured density distributions. The formation of an inhomogeneous distribution is discussed by a time-resolved analysis of the filling process. Grain rearrangement and densification during subsequent feeding shoe passages are characterized. The shoe velocity was tested for its influence on the density homogeneity. Suggestions for density homogenization with the application of cavity oscillations or volumetric filling are given. A density homogeneity index is introduced. The application of a coarse graining scheme circumvents the intrinsic difficulty of non-manageable grain numbers in 3D filling simulations. The validity and limitations of this scheme are discussed.

© 2009 Elsevier B.V. All rights reserved.

1. Introduction

Powder compaction and sintering [1] are important techniques for the mass production of geometrically complex parts. The standard processing route [2,3] starts with the die filling step. Powder is poured from a reservoir into the feeding shoe, which then passes the cavity one or more times thereby delivering powder into it. The next step is uniaxial compaction of the powder creating a relatively brittle green body. Finally, the green body is ejected from the cavity and sintered in a furnace where thermal activation below the melting point produces a fully dense structure [1]. Necks form and grow between adjacent grains thereby eliminating the porosity of the part.

Generally, the filling of the die and the subsequent compaction lead to inhomogeneous distributions of the powder in the green body [4,5]. Green density gradients yield inhomogeneous shrinkage during sintering and therefore distortions of the sintered part. Thus, it is desirable to identify mechanisms leading to density inhomogeneities during the die filling step. This knowledge can then be used to improve the overall filling homogeneity by appropriate process parameter adjustment. The objectives of fill density prediction and homogenization establish the motivation for the present study. In this regard a numerical approach is beneficial in two ways. First, density information is accessible at any spatial or temporal resolution. Second, variations of process parameters can be tested and analyzed with comparably little effort. In addition, calculated densities can directly be used as an initial condition for

compaction and sintering simulations in order to model the complete processing route [6].

Only few simulations of die filling can be found in the literature. Wu et al. [7,8] and Guo et al. [9,10] were the first to use the discrete element method (DEM) [11] for die filling simulations in order to investigate the influence of escaping air and cavity geometry. Riera et al. [12] modeled die filling using a scheme based on the finite element method. Gustafsson et al. [13] developed a smoothed particle hydrodynamics model for the same purpose. Common to these approaches is that they are restricted to two dimensions and, therefore, provide at most a generic understanding of the filling process. No studies incorporating a 3D description are known to the authors except for their recent publication [14].

In the present work 3D DEM simulations are used to predict and optimize density distributions in die filling. The individual model grains are either composed of several primary spheres to mimic the irregularity of commonly used industrial powders or represented by simple spheres. Parameters controlling friction and cohesion of the DEM model are adjusted to reproduce the filling behavior of iron based Distaloy AE powder. For validation, simulated density distributions in different cavities are compared with experimentally measured data by Burch et al. [4]. Access to trajectories of every grain within the simulations render two new ways of die filling assessment possible. First, the formation of an inhomogeneous density distribution is investigated using a time-resolved analysis of the filling stage for the narrow ring cavity. Second, the effect of subsequent shoe passages on grain displacement and surface densification is studied by means of displacement fields. A variety of process parameters are tested numerically for their influence on the final density distribution: Variations of the feeding shoe velocity are carried out. Linear

* Corresponding author. Tel.: +49 761 5142 347; fax: +49 761 5142 491.

E-mail addresses: claas.bierwisch@iwm.fraunhofer.de (C. Bierwisch),

michael.moseler@iwm.fraunhofer.de (M. Moseler).

URL: <http://www.iwm.fraunhofer.de> (M. Moseler).

oscillations are applied to either shoe or cavity during the filling process. Linear and rotational oscillations with different frequencies and amplitudes are applied to the cavity after the shoe passage. By using a moveable lower punch volumetric filling is investigated as an alternative die filling method.

An intrinsic difficulty of die filling simulations in 3D is the large number of grains involved. This challenge is resolved by using larger model grains. The application of certain scaling rules for the intergranular forces ensures that dynamic and static properties of the granular material are independent of the actual grain size except for boundary effects [14].

This article is organized as follows. The numerical method is explained in Section 2. A summary of the used model parameters, the adjustment procedure, and the coarse graining method are presented in Section 3. Section 4 contains the main results of the study. The discussion is given in Section 5. The article ends with a general conclusion in Section 6.

2. Simulation method

DEM calculations are used for all simulations in the present study. Pioneering work on the description of powders and grains using this approach was done by Cundall [11], Campbell [15], Walton [16], Haff [17], and Herrmann [18]. DEM is currently developing into a versatile simulation method for particulate materials such as rocks, sand, and powders [19]. The dynamic behavior of an ensemble of grains is governed by Newton's equations of motion,

$$m_k \dot{\mathbf{v}}_k = \mathbf{f}_k, \quad \dot{\mathbf{r}}_k = \mathbf{v}_k, \quad (1)$$

$$I_k \dot{\boldsymbol{\omega}}_k = \mathbf{t}_k, \quad (2)$$

where m_k is the mass, \mathbf{r}_k is the center of mass position, \mathbf{v}_k is the velocity, I_k is the inertia tensor, and $\boldsymbol{\omega}_k$ is the angular velocity of the grain with label k . The total force acting on the grain is \mathbf{f}_k while the total torque is \mathbf{t}_k . The grains interact via explicitly defined force laws and they can be affected by external forces such as gravity. Eqs. (1) and (2) are solved by explicit time integration using a velocity Verlet scheme [20] with fixed timestep Δt ,

$$\mathbf{r}_k(t + \Delta t) = \mathbf{r}_k(t) + \mathbf{v}_k(t)\Delta t + \frac{\mathbf{f}_k(t)\Delta t^2}{2m_k}, \quad (3)$$

$$\mathbf{v}_k(t + \Delta t) = \mathbf{v}_k(t) + \frac{(\mathbf{f}_k(t) + \mathbf{f}_k(t + \Delta t))\Delta t}{2m_k}, \quad (4)$$

$$\boldsymbol{\omega}_k(t + \Delta t) = \boldsymbol{\omega}_k(t) + \frac{I_k^{-1}(\mathbf{t}_k(t) + \mathbf{t}_k(t + \Delta t))\Delta t}{2}. \quad (5)$$

Fig. 1 shows DEM model grains and a picture of a typical iron powder grain. The brand name of the powder is Distaloy AE. A former study revealed that mimicking the shape of irregular grains—in contrast to simple spheres—is necessary in order to reproduce both static (e.g., angle of repose) and dynamic (e.g., flow rates) properties

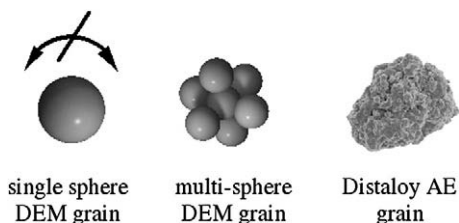


Fig. 1. DEM grains as used in the simulations and image of a real Distaloy AE grain.

[14]. The influence of the grain shape on flow rates was also stressed in previous numerical investigations on die filling in two dimensions [8,21]. In this work two DEM grain models were used. Mainly, a multi-sphere model was employed where a grain is composed of primary spheres which form the elementary objects. A similar approach using non-spherical grain shapes was first introduced to model granular heaps in two dimensions [22]. The primary spheres are rigidly connected, i.e., the grains have no vibrational degrees of freedom and cannot fracture. Although the morphology of the Distaloy AE grains is not covered in detail the model allows for inclusion of geometrical interlocking of different grains.

When two primary spheres of different grains come into contact, i.e., their surfaces touch, the forces acting on the spheres are calculated. The total force and torque acting on a grain is then given by summation over its primary spheres. The equations of motion are solved under the constraint of the stiffness of each grain. For this purpose a rigid body motion solver is used, which is based on a quaternion representation of the Euler angles of rotation [23]. The components of the inertia tensors I_k of the grains are obtained via summation over the constituent primary spheres,

$$(I_k)^{\alpha\beta} = \sum_i \left(\frac{2}{5} m_i R_i^2 \delta^{\alpha\beta} + m_i (\mathbf{b}_i^\alpha \delta^{\alpha\beta} - b_i^\alpha b_i^\beta) \right), \quad (6)$$

where a sphere with label i has mass m_i , radius R_i , and is located at $\mathbf{b}_i = (b_i^x, b_i^y, b_i^z)$ with respect to the center of mass of the composed grain. $\alpha, \beta \in (x, y, z)$ and $\delta^{\alpha\beta}$ is the Kronecker delta.

For comparison, simple spheres without rotational degrees of freedom were assessed as a second DEM grain model. It was found that its performance in describing a real powder comprehensively is inferior to the multi-sphere model while it is superior to a single sphere model with rotational degrees of freedom [14]. Of course, a single sphere model is computationally more efficient than a multi-sphere model.

2.1. Force laws

The primary spheres labeled i and j are described by the position vectors \mathbf{r}_{ij} , the velocities \mathbf{v}_{ij} , and the radii R_{ij} . During contact they undergo the deformation $h_{ij} = R_i + R_j - |\mathbf{r}_{ij}|$, $\mathbf{r}_{ij} = \mathbf{r}_i - \mathbf{r}_j$. No forces are applied if $h_{ij} < 0$.

Along the unit vector normal to the contact plane, $\hat{\mathbf{r}}_{ij} = \mathbf{r}_{ij}/|\mathbf{r}_{ij}|$, act three forces: elastic repulsion, cohesion, and viscous damping. Repulsion is taken to be of Hertzian type [24],

$$\mathbf{f}_{ij}^e = \left(\frac{2}{3} \tilde{E} \sqrt{R_{\text{eff}}} h_{ij}^{3/2} \right) \hat{\mathbf{r}}_{ij}. \quad (7)$$

$\tilde{E} = E/(1 - \nu^2)$, where E is Young's modulus, ν is Poisson's ratio, and $R_{\text{eff}} = R_i R_j / (R_i + R_j)$ is an effective radius. Cohesion is considered using the Johnson–Kendall–Roberts model [25],

$$\mathbf{f}_{ij}^{\text{coh}} = - \left(\sqrt{4\pi w \tilde{E}} R_{\text{eff}}^{3/4} h_{ij}^{3/4} \right) \hat{\mathbf{r}}_{ij}, \quad (8)$$

which is the natural extension of the Hertzian contact law upon introducing the free surface energy per unit area, $w/2$. Energy dissipation during the contact is described by a viscous force [26],

$$\mathbf{f}_{ij}^v = - \left(\gamma_n \sqrt{R_{\text{eff}}} h_{ij} \right) (\mathbf{v}_i - \mathbf{v}_j) \cdot \hat{\mathbf{r}}_{ij} \hat{\mathbf{r}}_{ij}, \quad (9)$$

where γ_n is an empirical damping parameter.

Static and sliding friction is modeled in the sense of Cundall and Strack [11]. An imaginary spring is applied at the initial contact points of the two primary spheres. The elongation ξ_{ij} of the spring is tracked during contact evolution. A restoring force acts at each contact point

Download English Version:

<https://daneshyari.com/en/article/238060>

Download Persian Version:

<https://daneshyari.com/article/238060>

[Daneshyari.com](https://daneshyari.com)